Pose Observers for Unmanned Air Vehicles

S. Brás, J. F. Vasconcelos, C. Silvestre and P. Oliveira

Abstract— This paper addresses the design and discrete time implementation of nonlinear observers for the estimation of position and attitude with application to Unmanned Air Vehicles. A continuous time nonlinear observer on SE(3) is derived, that uses inertial and ranges measurements. The estimation errors are shown to converge exponentially fast to the desired equilibrium points in the presence of bias in the rate gyros. An observer discrete time implementation is proposed that resorts to recent geometric numeric integration results suitable for solving ODEs on SO(3). Simulation results are presented to assess the performance of the continuous time observer and of the discrete time implementation. The estimation results in the presence of noise in the inertial and range measurements are also analyzed.

I. INTRODUCTION

Attitude and position estimation is a classical problem often subject to new advances and enriching insights, despite its wide historical background. Among a large diversity of estimation techniques, nonlinear observers stand out as a promising approach often endowed with stability results.

Research on the problem of deriving a stabilizing law for systems evolving on manifolds, where attitude is parameterized, can be found in [1], [2], [3], [4], [5], that provide important guidelines for observer design and discuss the topological characteristics and limitations for achieving global stabilization on the SO(3) manifold.

In many applications it is desired to design observers based only on the rigid body kinematics, that are an exact description of the physical quantities involved. In this approach, the attitude and position of the vehicle are propagated by integrating inertial sensor measurements [6], [7], [8],[9].

The development of numeric integration methods that preserve geometric properties, has witnessed in the last fifteen years a remarkable progress, and particular emphasis was placed by the scientific community on integration methods for integration of differential equations evolving on a Lie group. These methods were originally proposed by Crouch and Grossman in [10], and the general order conditions computed in [11]. In [12] the author construct generalized Runge-Kutta methods for integration of differential equations evolving on Lie groups, where the computations are performed in the Lie algebra, which is a linear space. More recently, the work in [13], [14] derives the commutator free Lie group method, to overcome some of the problems associated with the computation of commutators. An application

The authors are with the Institute for Systems and Robotics (ISR), Instituto Superior Técnico, Lisbon, Portugal. E-mails: {sbras, jfvasconcelos, cjs, pjcro}@isr.ist.utl.pt Tel: (+351) 21-8418054, Fax: (+351) 21-8418291.

of geometric numeric integration to multi-body dynamics evolving in SE(3) can be found in [15].

In this work, an attitude and position nonlinear observer is proposed, that integrates measurements from inertial sensors, namely accelerometers and rate gyros, with ranges provided by an acoustic positioning system. The latter is composed by an ultrasonic beacon array assumed fixed in the inertial frame and an acoustic receiver array installed on the vehicle. The range data supplied by the acoustic positioning system is processed resorting to a standard spherical interpolation technique that provides the positions of the beacons in vehicle frame, and the position of the receivers in the inertial frame. By exploiting sensor information, a stabilizing feedback law is proposed and the exponential convergence to the origin of the estimation errors is shown.

The discrete time implementation of the observer is addressed. Using recent results from numerical analysis, an integration method is adopted to approximate conveniently the original continuous time observer. The discrete time algorithm is detailed and its performance is illustrated in simulation. Discrete time implementation results, with noise in the inertial and range measurements, are presented to support that the algorithm can be adopted in practice.

The paper is structured as follows. In Section II, the attitude and position estimation problem is introduced. The sensors installed onboard the vehicle are described and some geometric relations are introduced. In Section III the attitude and position observers are proposed, and their properties are highlighted. A low complexity discrete time implementation of the observer is presented in Section IV, and in Section V simulations illustrate and compare the performance of the observer and its discrete time approximation. Simulation results with noisy sensors are also presented. Concluding remarks and future work are presented in Section VI.

NOMENCLATURE

The used notation is rather standard. The set of real $n \times m$ matrices is denoted as $M(n,m)$ and $M(n) := M(n,n)$. The set of orthogonal, and special orthonormal matrices are respectively denoted as $O(n) := \{U \in M(n) : U^T U = I\}$, $SO(n) := \{R \in O(n) : \det(R) = 1\}$. The n-dimensional sphere and ball are described by $S(n) := \{x \in \mathbb{R}^{n+1} : x^T x = 1\}$ and $B(n) := \{x \in \mathbb{R}^{n+1} : x^T x \leq 1\}$, respectively. The operator $[x]_\times$ stands for the skew symmetric matrix defined by the vector $x \in \mathbb{R}^3$ such that $[x]_\times y = x \times y$, $y \in \mathbb{R}^3$, and $[.]_\otimes$ denote the *unskew* operator, such that, $[[a]_\times]_\otimes = a$, $a \in \mathbb{R}^3$. The time dependence of variables will be omitted in general, but explicitly denoted where consider necessary.
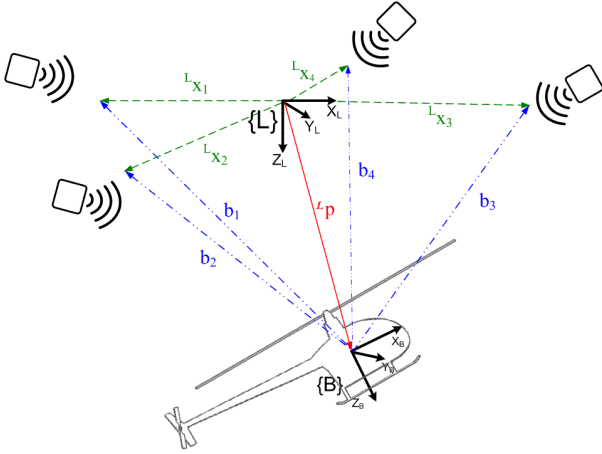
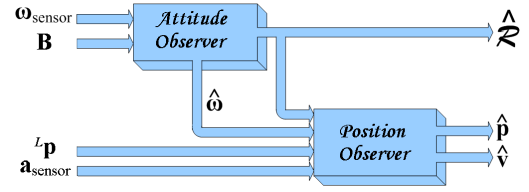Fig. 1.   Frames and navigation system configuration.

Fig. 2.   Cascaded observer, composed by the attitude and the position observers.

attitude observer that combines the inertial measurements with ranges between a beacon array and a receiver array.

III. OBSERVER SYNTHESIS

The proposed observer is designed to match the rigid body dynamics and, as illustrated in Fig. 2, it results in a cascaded composition, where the attitude and angular velocity estimates, from the attitude observer, are fed into the position observer. In this section the attitude and position observers are presented and their properties derived. It is shown that the attitude and angular velocity bias errors converge exponentially fast to the origin and that the position observer is globally exponentially stable.

A. Attitude Observer

The attitude observer considered in this section estimates the rotation matrix by exploiting angular velocity measurements available from rate gyros, and angular position data obtained from the receiver array installed on the vehicle. The proposed observer estimates the orientation of the rigid body by computing the kinematics

$$\dot{\hat{\mathcal{R}}} = \hat{\mathcal{R}} \left[\boldsymbol{\omega}^*\right]_\times, \tag{1}$$

where $\hat{\mathcal{R}}$ is the estimated attitude, and $\boldsymbol{\omega}^*$ is the feedback term that compensates for the estimation errors. See [6] and references therein for related work based on vector measurements. Whereas the angular velocity measurements, $\boldsymbol{\omega}_{sensor}$ are used directly in the observer term $\hat{\boldsymbol{\omega}}$, the beacons positions in frame $\{B\}$, $\mathbf{b}_i$, are introduced by means of a convenient linear coordinate transformation.

The attitude error is defined as $\tilde{\mathcal{R}} := \hat{\mathcal{R}}\mathcal{R}^T$ and its dynamics are given by $\dot{\tilde{\mathcal{R}}} = \tilde{\mathcal{R}} \left[\mathcal{R}(\boldsymbol{\omega}^* - \boldsymbol{\omega})\right]_\times$. The error matrix $\tilde{\mathcal{R}}$ can be parameterized in Euler angle-axis by a rotation vector $\boldsymbol{\lambda} \in \mathbb{S}(2)$ and by a rotation angle $\theta \in [0 \ \pi]$, yielding the formulation [17] $\tilde{\mathcal{R}} = \mathrm{rot}(\theta, \boldsymbol{\lambda}) := \cos(\theta)\mathbf{I} + \sin(\theta)\left[\boldsymbol{\lambda}\right]_\times + (1 - \cos(\theta))\boldsymbol{\lambda}\boldsymbol{\lambda}^T$.

Consider the transformation $^B\mathbf{U}_X := \mathbf{B}\mathbf{D}_X\mathbf{A}_X$, where $\mathbf{D}_X := \begin{bmatrix} \mathbf{0}_{1 \times n-1} \\ \mathbf{I}_{n-1} \end{bmatrix} - \begin{bmatrix} \mathbf{I}_{n-1} \\ \mathbf{0}_{1 \times n-1} \end{bmatrix}$ and $\mathbf{A}_X := [a_{ij}]$. The representation of the transformation in frame $\{L\}$, is given by $\mathbf{U}_X := \mathcal{R}^B\mathbf{U}_X = \mathbf{X}\mathbf{D}_X\mathbf{A}_X$.

Some rotational degrees of freedom are unobservable in the case beacons positions are all collinear as discussed in [6] and references therein. The following necessary condition is assumed.

Assumption 1: The positions of the beacons are not collinear, i.e. $\mathrm{rank}(\mathbf{B}) \geq 2$.

The directionality associated with the beacons positions is made uniform by defining transformation $\mathbf{A}_X$ such that

II. PROBLEM FORMULATION

This section, introduces the sensor suite used in the attitude and position observer. The rigid body kinematics are described by

$$\dot{\mathcal{R}} = \mathcal{R} \left[\boldsymbol{\omega}\right]_\times, \quad \dot{\mathbf{p}} = \mathbf{v} - \left[\boldsymbol{\omega}\right]_\times \mathbf{p}, \quad \dot{\mathbf{v}} = \mathbf{a}_{\mathrm{SF}} + \mathcal{R}^{T \, L}\mathbf{g} - \left[\boldsymbol{\omega}\right]_\times \mathbf{v},$$

where $\mathcal{R}$ is the shorthand notation for the rotation matrix from body frame $\{B\}$ to the local frame $\{L\}$, $\boldsymbol{\omega}$ is the rigid body angular velocity expressed in $\{B\}$, $\mathbf{p}$, and $\mathbf{v}$ are the position and velocity of the rigid body with respect to $\{L\}$ expressed in $\{B\}$, respectively, $^L\mathbf{g}$ is the gravitational acceleration expressed in $\{L\}$, and $\mathbf{a}_{\mathrm{SF}}$ is the specific force applied to the vehicle expressed in $\{B\}$. For the sake of simplicity, $\{L\}$ is assumed to be an inertial frame.

The rigid body angular velocity is measured by a rate gyro sensor triad, corrupted by a constant bias term

$$\boldsymbol{\omega}_{sensor} = \boldsymbol{\omega} + \mathbf{b}_\omega,$$

and a triaxial accelerometer measures the specific force, which is the difference between the vehicle acceleration $^B\mathbf{a}$ and the gravitational acceleration $^B\mathbf{g}$, both in expressed in body frame,

$$\mathbf{a}_{\mathrm{SF}} := \mathbf{a}_{sensor} = {}^B\mathbf{a} - {}^B\mathbf{g}.$$

The acoustic positioning system gives the range from each of the beacons to the acoustic receivers installed on the vehicle. Using a spherical interpolation method [16], it is possible to obtain the position of receiver j in $\{L\}$, denoted as $^L\mathbf{p}_j$, and the position of beacon i in $\{B\}$, denoted as $\mathbf{b}_i$. Without loss of generality, the origin of $\{B\}$ is defined at receiver 1, i.e. $^L\mathbf{p} = {}^L\mathbf{p}_1$. The position of the beacons in $\{B\}$ is described by $\mathbf{b}_i = \mathcal{R}^T \left({}^L\mathbf{x}_i - {}^L\mathbf{p}\right)$, where $i = 1, ..., n$, n is the number of beacons and $^L\mathbf{x}_i$ is the position of the i-*th* beacon in $\{L\}$. This relationship can be expressed in matrix from as $\mathbf{B} = \mathcal{R}^T(\mathbf{X} - {}^L\mathbf{p}\mathbf{1}_n^T)$, where $\mathbf{B} := [\mathbf{b}_1 ... \mathbf{b}_n]$, $\mathbf{X} := [{}^L\mathbf{x}_1 ... {}^L\mathbf{x}_n]$, $\mathbf{B}$, $\mathbf{X} \in \mathrm{M}(3, n)$ and $\mathbf{1}_n := [1 ... 1]^T$.

The origin of the local frame is defined at the centroid of beacons. Therefore, the vectors $^L\mathbf{x}_i$, $i = 1, ..., n$, illustrated in Fig. 1, verify $\sum_{i=1}^n {}^L\mathbf{x}_i = 0$.

The objective of the present work is to exploit the information provided by the sensor suite, by deriving a position and

$\mathbf{U}_X \mathbf{U}_X^T = \mathbf{I}$. The desired $\mathbf{A}_X$ exists if Assumption 1 is satisfied, nevertheless the case of two noncollinear beacons positions requires minor modifications of the feedback law, see [6, Appendix A] for discussion of this subject.

Let the bias in angular velocity measurements be constant, i.e. $\dot{\mathbf{b}}_\omega = \mathbf{0}$, and consider the candidate Lyapunov function

$$V = 2(1 - \cos(\theta)) + \frac{1}{2K_{b_\omega}}||\tilde{\mathbf{b}}_\omega||^2, \qquad (2)$$

where $K_{b_\omega} \in \mathbb{R}^+$, $\tilde{\mathbf{b}}_\omega := \hat{\mathbf{b}}_\omega - \mathbf{b}_\omega$, and $\hat{\mathbf{b}}_\omega$ is the estimated bias in angular velocity measurements. Its time derivative is given by

$$\dot{V} = \mathbf{s}_\omega^T(\boldsymbol{\omega}^* - \boldsymbol{\omega}) + \frac{1}{K_{b_\omega}}\dot{\tilde{\mathbf{b}}}_\omega^T \tilde{\mathbf{b}}_\omega, \qquad (3)$$

where $\mathbf{s}_\omega = \mathcal{R}^T \left[\tilde{\mathcal{R}} - \tilde{\mathcal{R}}^T \right]_\otimes = 2\sin(\theta)\mathcal{R}^T \boldsymbol{\lambda}$. The feedback term $\mathbf{s}_\omega$ can be expressed as an explicit function of the sensor readings [6, Theorem 8]

$$\mathbf{s}_\omega = \sum_{i=0}^{n} (\hat{\mathcal{R}}^T \mathbf{X} \mathbf{D}_X \mathbf{A}_X \mathbf{e}_i) \times (\mathbf{B} \mathbf{D}_X \mathbf{A}_X \mathbf{e}_i),$$

where n is the beacon number and $\mathbf{e}_i$ is the unit vector where $e_i=1$. The attitude feedback law is given by

$$\boldsymbol{\omega}^* = \boldsymbol{\omega}_{sensor} - \hat{\mathbf{b}}_\omega - K_\omega \mathbf{s}_\omega = \boldsymbol{\omega} - \tilde{\mathbf{b}}_\omega - K_\omega \mathbf{s}_\omega, \quad (4)$$

where $K_\omega \in \mathbb{R}^+$. Applying the feedback law (4) to the Lyapunov function (3) and defining

$$\dot{\hat{\mathbf{b}}}_\omega := K_{b_\omega} \mathbf{s}_\omega, \qquad (5)$$

the Lyapunov function derivative is given by $\dot{V}_b = -K_\omega ||\mathbf{s}_\omega||^2$.

Using the feedback law (4) and the definition (5) the closed loop attitude error dynamics results in

$$\dot{\tilde{\mathcal{R}}} = -K_\omega \tilde{\mathcal{R}}(\tilde{\mathcal{R}} - \tilde{\mathcal{R}}^T) - \tilde{\mathcal{R}} \left[\mathcal{R} \tilde{\mathbf{b}}_\omega \right]_\times$$
$$\dot{\hat{\mathbf{b}}}_\omega = K_{b_\omega} \mathcal{R}^T \left[\tilde{\mathcal{R}} - \tilde{\mathcal{R}}^T \right]_\otimes \qquad (6)$$

Global asymptotic stability of the origin is precluded by topological limitations associated with the estimation error $\tilde{\mathcal{R}} = \mathrm{rot}(\pi, \boldsymbol{\lambda})$ [18]. In the next lemma the boundedness of estimation errors is shown and used to provide sufficient conditions that exclude convergence to the equilibrium points satisfying $\tilde{\mathcal{R}} = \mathrm{rot}(\pi, \boldsymbol{\lambda})$.

Lemma 1: The estimation errors $\tilde{\mathbf{x}}_b = (\tilde{\mathcal{R}}, \tilde{\mathbf{b}}_\omega)$ are bounded. For any initial condition that verifies

$$\frac{\frac{1}{K_{b_\omega}}||\tilde{\mathbf{b}}_\omega(t_0)||^2}{4(1 + \cos(\theta(t_0)))} < 1, \qquad (7)$$

the attitude error is bounded by $\theta(t) \leq \theta_{\max} < \pi$ for all $t \geq t_0$.

Proof: Let $\Omega_\rho = \{\tilde{\mathbf{x}}_b \in D_b : V \leq \rho\}$. As the Lyapunov function (2) is a weighted distance from the origin, $\exists_\gamma ||\tilde{\mathbf{x}}_b||^2 \leq \gamma V$ and Ω_ρ is a compact set. $\dot{V} \leq 0$ implies that any trajectory that starts in Ω_ρ remains in Ω_ρ. So, $\forall_{t \geq t_0}||\tilde{\mathbf{x}}_b(t)||^2 \leq \gamma V(\tilde{\mathbf{x}}_b(t_0))$ and the state is bounded.

The gain condition (7) is equivalent to $V(\tilde{\mathbf{x}}_b(t_0)) < 4$. The invariance of Ω_ρ implies that $V(\tilde{\mathbf{x}}_b(t)) \leq V(\tilde{\mathbf{x}}_b(t_0))$,

and so $2(1 + \cos(\theta)) \leq V(\tilde{\mathbf{x}}_b(t_0)) < 4$ and consequently $\exists_{\theta_{\max}} : \theta(t) \leq \theta_{\max} < \pi \ \forall_{t \geq t_0}$. ∎

Exponential convergence of the system (6) trajectories to the desired equilibrium point is established in the following theorem.

Theorem 1: Assume that $\boldsymbol{\omega}$ is bounded. Then the attitude error and the bias estimation error converge exponentially fast to the equilibrium point $(\tilde{\mathcal{R}}, \tilde{\mathbf{b}}_\omega) = (\mathbf{I}, 0)$, for any initial condition satisfying (7).

Due to space constraints, the proof is omitted, but can be obtained by adaptation of the derivation used in [6, Theorem 7]

B. Position Observer

This section derives the position observer based on the IMU acceleration measurements, position readings obtained from range data, and on the attitude observer estimates. The dynamics of the position and velocity estimates are described by

$$\dot{\hat{\mathbf{p}}} = \hat{\mathbf{v}} - [\hat{\boldsymbol{\omega}}]_\times \hat{\mathbf{p}} + \mathbf{s}_p, \qquad (8)$$
$$\dot{\hat{\mathbf{v}}} = \mathbf{a}_{SF} + \hat{\mathcal{R}}^{TL}\mathbf{g} - [\hat{\boldsymbol{\omega}}]_\times \hat{\mathbf{v}} + \mathbf{s}_v, \qquad (9)$$

where $\mathbf{s}_p$ and $\mathbf{s}_v$ are the feedback terms that compensate for the estimation errors, and $\hat{\boldsymbol{\omega}}$ is an estimate of the angular velocity given by $\hat{\boldsymbol{\omega}} := \boldsymbol{\omega}_{sensor} - \hat{\mathbf{b}}_\omega = \boldsymbol{\omega} - \tilde{\mathbf{b}}_\omega$.

The feedback laws are obtain by setting $\mathbf{s}_p$ and $\mathbf{s}_v$ as

$$\mathbf{s}_p = -K_p(\hat{\mathbf{p}} - \hat{\mathcal{R}}^{TL}\mathbf{p}) \quad \mathbf{s}_v = -K_v(\hat{\mathbf{p}} - \hat{\mathcal{R}}^{TL}\mathbf{p}),$$

where $^L\mathbf{p}$ is the position of the origin of $\{B\}$, relatively to $\{L\}$, expressed in $\{L\}$.

The position and velocity errors are defined as $\tilde{\mathbf{p}} := \hat{\mathbf{p}} - \mathbf{p}$ and $\tilde{\mathbf{v}} := \hat{\mathbf{v}} - \mathbf{v}$, respectively. Their dynamics are given by

$$\dot{\tilde{\mathbf{p}}} = \tilde{\mathbf{v}} - [\hat{\boldsymbol{\omega}}]_\times \tilde{\mathbf{p}} + \left[\tilde{\mathbf{b}}_\omega \right]_\times \mathbf{p} - K_p(\hat{\mathbf{p}} - \hat{\mathcal{R}}^{TL}\mathbf{p})$$
$$\dot{\tilde{\mathbf{v}}} = (\hat{\mathcal{R}} - \mathcal{R})^{TL}\mathbf{g} - [\hat{\boldsymbol{\omega}}]_\times \tilde{\mathbf{v}} + \left[\tilde{\mathbf{b}}_\omega \right]_\times \mathbf{v} - K_v(\hat{\mathbf{p}} - \hat{\mathcal{R}}^{TL}\mathbf{p}). \qquad (10)$$

The stability of the system (10) is obtained by assuming a weak upper bound on the position and velocity trajectories.

Assumption 2: For any $\gamma_v, \gamma_p > 0$, there exist $k_v, k_p > 0$, such that vehicle position and velocity satisfy

$$||\mathbf{p}(t)|| \leq k_p e^{\gamma_p(t-t_0)}, \quad ||\mathbf{v}(t)|| \leq k_v e^{\gamma_v(t-t_0)}.$$

This assumption considers that the position and velocity cannot grow exponentially fast indefinitely, and is not restrictive in practice due to the fact that it is trivially verified by physical constraints.

By applying a convenient Lyapunov transformation, it can be shown that the attitude and position estimation errors converge exponentially fast to the origin. This is formally stated in the next theorem.

Theorem 2: Let Assumption 2 and the conditions of Theorem 1 be satisfied. Then the estimation errors converge exponentially fast to the equilibrium point $(\tilde{\mathcal{R}}, \tilde{\mathbf{b}}_\omega, \tilde{\mathbf{p}}, \tilde{\mathbf{v}}) = (\mathbf{I}, \mathbf{0}, \mathbf{0}, \mathbf{0})$ for any initial condition satisfying (7) and $(\tilde{\mathbf{p}}, \tilde{\mathbf{v}}) \in \mathbb{R}^3 \times \mathbb{R}^3$. Also, if $\mathcal{R}$ and $\mathbf{b}_\omega$ are known, the origin of (10) is globally exponentially stable.

Proof: Notice that $\hat{\mathbf{p}} - \hat{\mathcal{R}}^{TL}\mathbf{p} = \tilde{\mathbf{p}} + \mathcal{R}^T(\mathbf{I} - \tilde{\mathcal{R}}^T)\mathcal{R}\mathbf{p}$, and consider the Lyapunov transformation $\tilde{\mathcal{R}} \in SO(3)$

applied to vectors $\tilde{\mathbf{p}}$, and $\tilde{\mathbf{v}}$, where $\dot{\breve{\mathcal{R}}} = \breve{\mathcal{R}}\,[\hat{\boldsymbol{\omega}}]_{\times}$. The dynamics of the transformed system are given by

$$\frac{d}{dt}(\breve{\mathcal{R}}\tilde{\mathbf{p}}) = \breve{\mathcal{R}}\tilde{\mathbf{v}} - K_p\breve{\mathcal{R}}\tilde{\mathbf{p}} + \breve{\mathcal{R}}\tilde{\mathbf{b}}_\omega \mathbf{p} - K_p\breve{\mathcal{R}}\mathcal{R}\mathcal{R}^T\left(\mathbf{I}-\tilde{\mathcal{R}}\right)\mathcal{R}\mathbf{p}$$

$$\frac{d}{dt}(\breve{\mathcal{R}}\tilde{\mathbf{v}}) = \breve{\mathcal{R}}(\tilde{\mathcal{R}}^T-\mathbf{I})^L\bar{\mathbf{g}} - K_v\breve{\mathcal{R}}\tilde{\mathbf{p}} + \breve{\mathcal{R}}\tilde{\mathbf{b}}_\omega\mathbf{v}$$
$$- K_v\breve{\mathcal{R}}\mathcal{R}^T(\mathbf{I}-\tilde{\mathcal{R}})\mathcal{R}\mathbf{p},$$

which can be rewritten in matrix form as

$$\dot{\boldsymbol{\xi}} = A\boldsymbol{\xi} + \mathbf{u} \qquad (11)$$

where $\boldsymbol{\xi} = \begin{bmatrix} \breve{\mathcal{R}} & \mathbf{0} \\ \mathbf{0} & \breve{\mathcal{R}} \end{bmatrix}\mathbf{x}$, with $\mathbf{x} = \begin{bmatrix} \tilde{\mathbf{p}}^T & \tilde{\mathbf{v}}^T \end{bmatrix}^T$, $A = \begin{bmatrix} -K_p\mathbf{I} & \mathbf{I} \\ -K_v\mathbf{I} & \mathbf{0} \end{bmatrix}$, and $\mathbf{u} = \begin{bmatrix} \breve{\mathcal{R}}\tilde{\mathbf{b}}_\omega\mathbf{p} - K_p\breve{\mathcal{R}}\mathcal{R}^T\left(\mathbf{I}-\tilde{\mathcal{R}}\right)\mathcal{R}\mathbf{p} \\ \breve{\mathcal{R}}\tilde{\mathbf{b}}_\omega\mathbf{v} - K_v\breve{\mathcal{R}}\mathcal{R}^T\left(\mathbf{I}-\tilde{\mathcal{R}}\right)\mathcal{R}\mathbf{p} + \breve{\mathcal{R}}(\hat{\mathcal{R}}-\mathcal{R})^{T L}\bar{\mathbf{g}} \end{bmatrix}$. The system (11) is linear time invariant and for $K_p > 0$ and $K_v > 0$ the matrix A is Hurwitz, therefore the system is stable.

From Theorem 1 is known that for K_{b_ω} large enough, there are $k_{\mathcal{R}}, k_b, \gamma_{\mathcal{R}}, \gamma_b > 0$ such that $||\tilde{\mathcal{R}}(t) - \mathbf{I}|| \leq k_{\mathcal{R}}||\tilde{\mathcal{R}}(t_0) - \mathbf{I}||e^{-\gamma_{\mathcal{R}}(t-t_0)}$, $||\tilde{\mathbf{b}}_\omega(t)|| \leq k_b||\tilde{\mathbf{b}}_\omega(t_0)||e^{-\gamma_b(t-t_0)}$. The input vector $||\mathbf{u}||$ verifies the following inequality

$$||\mathbf{u}|| \leq ||\tilde{\mathbf{b}}_\omega||\,(||\mathbf{p}|| + ||\mathbf{v}||) + \left|\left|\tilde{\mathcal{R}} - \mathbf{I}\right|\right|\left((K_p + K_v)||\mathbf{p}|| + ||^L\bar{\mathbf{g}}||\right).$$

Using the fact that $||\bar{\mathbf{p}}(t)||$ and $||\bar{\mathbf{v}}(t)||$ satisfy Assumption 2, it can be shown that $||\mathbf{u}(t)|| \leq k_u e^{-\gamma_u(t-t_0)}$, where $k_u = k_b(k_p + k_v)||\tilde{\mathbf{b}}_\omega(t_0)|| + k_{\mathcal{R}}\left(k_p(K_p + K_v) + ||^L\mathbf{g}||\right)||\mathcal{R}(t_0) - \mathbf{I}||$ and $\gamma_u = \min\{\gamma_b - \max\{\gamma_p, \gamma_v\}, \gamma_{\mathcal{R}} - \gamma_p\}$, that is positive since γ_p and γ_v can be made as small as desired by Assumption 2. The transformed state $\boldsymbol{\xi}(t)$ satisfies

$$\boldsymbol{\xi}(t) = e^{A(t-t_0)}\boldsymbol{\xi}(t_0) + \int_{t_0}^{t} e^{A(t-\tau)}\mathbf{u}(\tau)d\tau,$$

and by [19] the stability of the origin implies that there exists $k_a, \gamma_a > 0$ such that $||e^{At}|| \leq k_a e^{-\gamma_a t}$, therefore the subsequent inequality holds

$$||\boldsymbol{\xi}(t)|| \leq k_a e^{-\gamma_a(t-t_0)}||\boldsymbol{\xi}(t_0)|| + k_a k_u \int_{t_0}^{t} e^{-\gamma_a(t-\tau)-\gamma_u(\tau-t_0)}d\tau$$

$$\leq 2\max\left\{k_a||\boldsymbol{\xi}(t_0)||, \frac{k_a k_u}{|\gamma_a - \gamma_u|}\right\}e^{-\min\{\gamma_u,\gamma_a\}(t-t_0)}.$$

Concatenating the attitude and transformed position estimation errors as $\mathbf{x}_f := (\tilde{\mathcal{R}} - \mathbf{I}, \tilde{\mathbf{b}}_\omega, \boldsymbol{\xi})$ and using the inequalities $||\mathbf{x}_f|| \leq ||\tilde{\mathcal{R}} - \mathbf{I}|| + ||\tilde{\mathbf{b}}_\omega|| + ||\boldsymbol{\xi}||$ and $\max\{||\tilde{\mathcal{R}} - \mathbf{I}||, ||\tilde{\mathbf{b}}_\omega||, ||\boldsymbol{\xi}||\} \leq ||\mathbf{x}_f||$, an exponential upper bound is given by

$$||\mathbf{x}_f(t)|| \leq k_{\max}||\mathbf{x}_f(t_0)||e^{-\gamma_{\min}(t-t_0)},$$

where $k_{\max} = k_{\mathcal{R}} + k_b + k_a + k_a \frac{k_b(k_p + k_v + k_{\mathcal{R}} k_p(K_p + K_v) + k_{\mathcal{R}}||^L\mathbf{g}||)}{|\gamma_a - \gamma_u|}$ and $\gamma_{\min} = \min\{\gamma_a, \gamma_b - \max\{\gamma_p, \gamma_v\}, \gamma_{\mathcal{R}} - \gamma_p\}$.

Hence, the trajectories of the system (6,11) converge exponentially fast to the origin. The fact that $||\boldsymbol{\xi}(t)|| = ||\mathbf{x}(t)||$ bears the exponential convergence of cascaded observer (6,10). If $\mathcal{R}$ and $\mathbf{b}_\omega$ are known, then $\mathbf{u}(t) = \mathbf{0}$ and the origin of (11) is globally exponentially stable by the properties of linear time-invariant systems. ∎

IV. OBSERVER DISCRETE TIME IMPLEMENTATION

This section presents a discrete time implementation of the pose observer proposed in Section III. This implementation will be obtained by applying numeric integration methods to the observer continuous time dynamics. The integration method should guarantee that the discrete time implementation approximates conveniently the original continuous time observer. The selection of the method depends on the quality of the sensor suite, the desired sampling rate and the computational resources available.

A. Numeric Integration of the Attitude Observer

The attitude observer dynamics is composed by differential equations (1) and (5), evolving in SO(3) and $\mathbb{R}^3$, respectively. The first is integrated resorting to a geometric numeric integration namely, the Crouch-Grossman Method (CG) [10], the Munthe-Kaas Method (MK) [12], and the Commutator-Free Lie group Method (CF) [13]. The second is implemented in discrete time using a classical numeric integration technique.

The equation (1) of observer dynamics is not in the general form $\dot{Y} = A(t, Y)Y$, which is assumed in the referenced geometric integration methods, nonetheless an equivalent equation in the desired form can be obtained by transposing (1) which gives $(\dot{\hat{\mathcal{R}}})^T = (\hat{\mathcal{R}}\,[\boldsymbol{\omega}^*]_\times)^T \Leftrightarrow \dot{\hat{\mathcal{R}}}^T = -[\boldsymbol{\omega}^*]_\times \hat{\mathcal{R}}^T$.

The presented geometric numerical integration algorithms require the knowledge of the function $\boldsymbol{\omega}^*(t)$ in instants between sampling times. Different sampling and computation strategies can be adopted to obtain an approximation of this function using methods such as polynomial interpolation of the sampled data. In the present research project, where the unit is equipped with tactical grade inertial sensors and computational resources are limited, $\boldsymbol{\omega}^*$ is linearly interpolated in the interval $[(k-1)T, kT]$.

To implement (1), a second order integration method is adopted. Note that higher order methods do not enhance the results accuracy, due to the linear interpolation adopted for $\boldsymbol{\omega}^*$. The complexity required to implement each step of the second order CG and MK methods is summarized in Table I, for the operations in SO(3) exponential map (Exp), inverse of differential of the exponential map (Dexp^{-1}), and 3×3 matrix multiplication (mmult), as defined in [15]. Note that Exp and Dexp^{-1} have close form solutions on the rotation group. The CF methods were derived for order $>= 3$ and therefore they are not included.

TABLE I
COMPLEXITY IN EACH STEP FOR CG, MK AND LC METHODS.

operation	Exp	Dexp^{-1}	mmult
CG 2$^{\text{nd}}$ order	1	0	1
MK 2$^{\text{nd}}$ order	1	1	2

The discrete time implementation of equation (5) was obtained by using a second order *Adams-Moulton Method*, see [20] for further details. This selection was done based on similar arguments as those used for (1). The resulting attitude observer numerical integration algorithm can be summarized as

$$\hat{\mathbf{b}}_{\omega\,k} = \hat{\mathbf{b}}_{\omega\,k-1} + \frac{T}{2}\left(K_{b_\omega}\mathbf{s}_{\omega\,k} + K_{b_\omega}\mathbf{s}_{\omega\,k-1}\right)$$

$$K^{(1)} = -(\boldsymbol{\omega}^*(kT - T/2)), \quad \hat{\mathcal{R}}_k^T = \text{Exp}\left(TK^{(1)}\right)\hat{\mathcal{R}}_{k-1}^T,$$

$$\mathbf{s}_{\omega\,k} = \sum_{i=0}^{n}(\hat{\mathcal{R}}_k^T\mathbf{X}\mathbf{D}_X\mathbf{A}_X\mathbf{e}_i) \times (\mathbf{B}_k\mathbf{D}_X\mathbf{A}_X\mathbf{e}_i).$$

Since this is an implicit algorithm a numeric technique like the *Fixed-Point Method* should be run in each integration step.

B. Numeric Integration of the Position Observer

The numerical integration of the differential equations associated to the position observer, (8) and (9), both evolving in $\mathbb{R}^3$, was performed by resorting to a second order *Adams-Moulton Method*. The resulting numerical integration algorithm is described as follows

$$g_{p\ k} = \hat{\mathbf{v}}_k - [\hat{\boldsymbol{\omega}}_k]_\times \hat{\mathbf{p}}_k - K_p(\hat{\mathbf{p}}_k - \hat{\mathcal{R}}_k^{TL}\mathbf{p}_k)$$

$$\hat{\mathbf{p}}_k = \hat{\mathbf{p}}_{k-1} + \frac{T}{2}(g_{p\ k} + g_{p\ k-1})$$

$$g_{v\ k} = \mathbf{a}_{\mathrm{SF}\ k} + \hat{\mathcal{R}}_k^{TL}\mathbf{g} - [\hat{\boldsymbol{\omega}}_k]_\times \hat{\mathbf{v}}_k - K_v(\hat{\mathbf{p}}_k - \hat{\mathcal{R}}_k^{TL}\mathbf{p}_k)$$

$$\hat{\mathbf{v}}_k = \hat{\mathbf{v}}_{k-1} + \frac{T}{2}(g_{v\ k} + g_{v\ k-1}).$$

This is also an implicit algorithm and therefore requires to be solved by a numeric method at each integration step.

V. SIMULATIONS

In this section, simulation results obtained for the continuous time observer and for its discrete time implementation are presented and discussed. Additional simulations illustrating the robustness of the discrete time implementation when the sensor readings are corrupted by Gaussian noise. The sampling frequency of the discrete implementation was set to 50 Hz. Five beacons were placed in the mission scenario located at $^L\mathbf{x}_1 = [20\ 20\ 20]^T$ m, $^L\mathbf{x}_2 = [-20\ -20\ 20]^T$ m, $^L\mathbf{x}_3 = [20\ -20\ -20]^T$ m, $^L\mathbf{x}_4 = [-20\ 20\ -20]^T$ m, and $^L\mathbf{x}_5 = [0\ 0\ 0]^T$ m. The acoustic receivers were placed onboard the vehicle at $^B\mathbf{r}_1 = [0\ 0\ 0]^T$ m, $^B\mathbf{r}_2 = [0.5\ 0\ 0]^T$ m, $^B\mathbf{r}_3 = [0\ 0.5\ 0]^T$ m, and $^B\mathbf{r}_4 = [0\ 0\ 0.5]^T$ m, where $^B\mathbf{r}_i$ denotes the position of the acoustic receiver i in body frame. The vehicle trajectory is characterized by oscillatory acceleration and angular velocity with frequency 0.5 Hz. The acceleration and angular velocity amplitudes are 1 m s^{-1}, and 1 rad s^{-1} in all axes, respectively.

The feedback gains were set to $K_\omega = 0.1$, $K_{b_\omega} = 0.003$, $K_p = 3$, and $K_v = 2$. The initial errors were assumed as $\tilde{\mathbf{p}}(t_0) = [0.5\ 0.5\ 0.5]^T$ m, $\tilde{\mathbf{v}}(t_0) = [0.5\ 0.5\ 0.5]^T$ m s^{-1}, $\theta(t_0) = 22.5\frac{\pi}{180}$ rad, and $\tilde{\mathbf{b}}_\omega(t_0) = \frac{\pi}{180}[-0.5\ -0.5\ -0.5]^T$ rad s^{-1}. The condition (7), that is $\frac{\frac{1}{K_{b_\omega}}||\tilde{\mathbf{b}}_\omega(t_0)||^2}{4(1+\cos(\theta(t_0)))} \approx 0.0206 < 1$ is verified. In the simulations with noise the standard deviations of accelerometers and rate gyros were set as $\sigma_a = 6 \times 10^{-3}$ m s^{-2} and $\sigma_\omega = 3.5 \times 10^{-4}$ rad s^{-1} in each channel, respectively, and the standard deviation for each measured range was $\sigma_{ranges} = 0.05$ m.

Fig. 3 illustrates the estimation errors of the continuous time observer and of its discrete time implementation. The angular velocity bias error decreases much slower than the other errors because K_{b_ω} is much smaller than the other gains. This is coherent with the fact that in practice the bias has lower bandwidth than the other quantities that are estimated. The quality of the discrete time approximation can be inferred from Fig. 4, where the differences between the continuous and discrete time observer estimates are depicted. The results of the simulation with noisy sensors are illustrated in Fig. 5 and Fig. 6. The latter figure also shows the position obtained by the acoustic positioning system, and
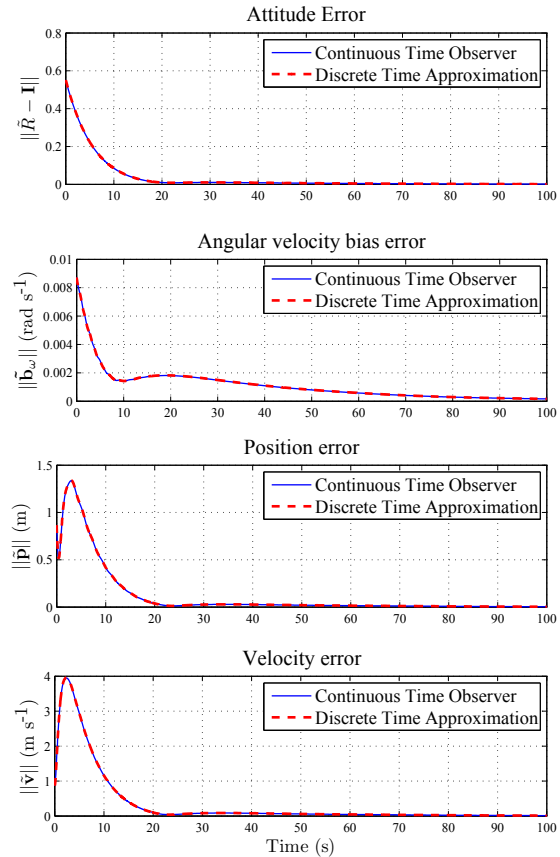

Fig. 3. Continuous observer and discrete time implementation estimates.

it can be seen that the discrete time implementation provides a better position estimate than that obtained using only the range measurement.

VI. CONCLUSIONS

In this work, a nonlinear attitude and position observer using inertial sensor measurements and ranges to acoustic beacons was derived. Using a cascade topology, it was shown that the attitude and position estimation errors converge exponentially fast to the origin. Existence of static bias in angular velocity measurements was considered. A method to obtain a discrete time implementation of the attitude observer using recent results from numeric integration in Lie groups was proposed, and a discrete implementation of the attitude and position observers was obtained. Simulations results demonstrated the convergence to the origin of the estimation errors. The good approximation brought about by the adopted discrete time algorithm evidenced that it is suitable for realistic applications. The performance of the discrete time implementation with noisy sensors provided further motivation to its development and implementation. Future work will focus on the implementation and validation of the proposed algorithm in a real time architecture onboard an Unmanned Aerial Vehicle.

REFERENCES

[1] N. Chaturvedi and N. McClamroch, "Almost global attitude stabilization of an orbiting satellite including gravity gradient and control
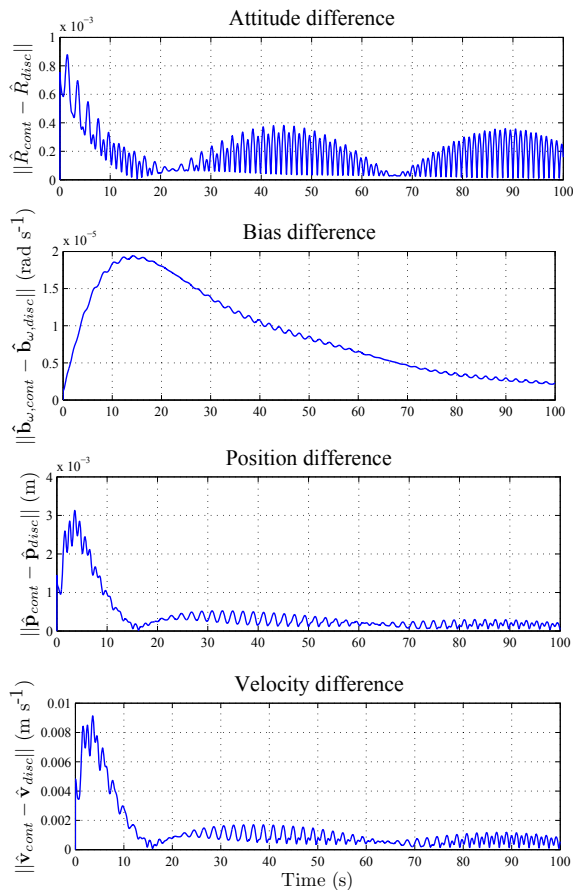
Fig. 4. Difference between the estimates of the continuous and discrete time implementation.
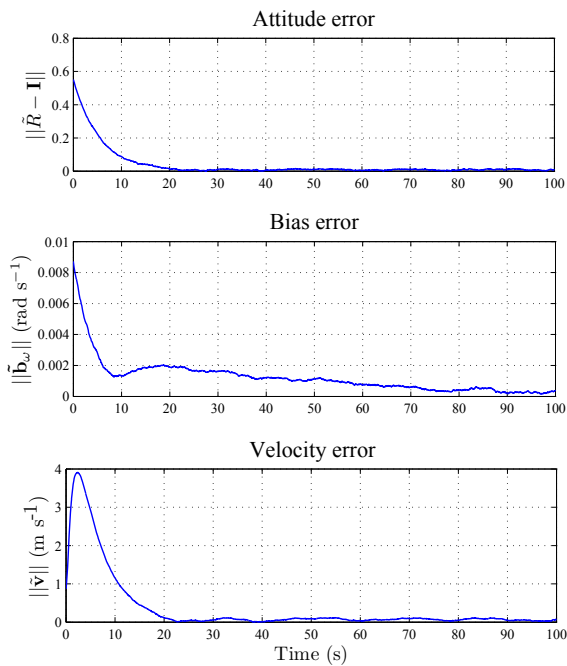

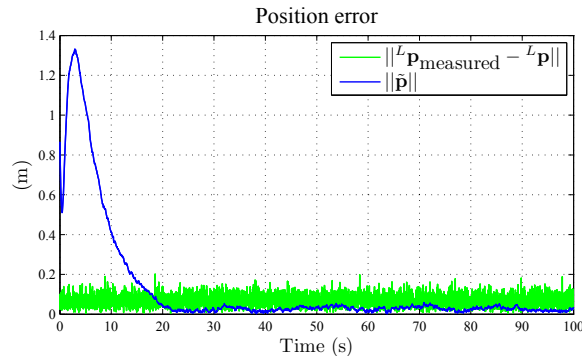Fig. 5. Estimation errors using noisy sensors.

Fig. 6. Position estimates of observer discrete time implementation and of the acoustic positioning system using noisy sensors.

saturation effects," in *2006 American Control Conference*, Minnesota, USA, Jun. 2006.

[2] D. Fragopoulos and M. Innocenti, "Stability considerations in quaternion attitude control using discontinuous Lyapunov functions," *IEEE Proceedings on Control Theory and Applications*, vol. 151, no. 3, pp. 253– 258, May 2004.

[3] D. E. Koditschek, "The Application of Total Energy as a Lyapunov Function for Mechanical Control Systems," *Control Theory and Multibody Systems*, vol. 97, pp. 131–151, 1989.

[4] M. Malisoff, M. Krichman, and E. Sontag, "Global stabilization for systems evolving on manifolds," *Journal of Dynamical and Control Systems*, vol. 12, no. 2, pp. 161–184, Apr. 2006.

[5] S. Salcudean, "A globally convergent angular velocity observer for rigid body motion," *IEEE Transactions on Automatic Control*, vol. 36, no. 12, pp. 1493–1497, Dec. 1991.

[6] J. Vasconcelos, R. Cunha, C. Silvestre, and P. Oliveira, "A landmark based nonlinear observer for attitude and position estimation with bias compensation," in *17th IFAC World Congress*, South Korea, Seoul, Jul. 2008.

[7] P. Batista, C. Silvestre, and P. Oliveira, "Position and velocity navigation filters for marine vehicles," in *17th IFAC World Congress*, South Korea, Seoul, Jul. 2008.

[8] R. Mahony, T. Hamel, and J. Pflimlin, "Non-linear complementary filters on the Special Orthogonal Group," *IEEE Transactions on Automatic Control*, vol. 53, no. 5, pp. 1203–1218, Jun. 2008.

[9] J. Thienel and R. M. Sanner, "A coupled nonlinear spacecraft attitude controller and observer with an unknown constant gyro bias and gyro noise," *IEEE Transactions on Automatic Control*, vol. 48, no. 11, pp. 2011–2015, Nov. 2003.

[10] P. E. Crouch and R. Grossman, "Numerical integration of ordinary differential equations on manifolds," *J. Nonlinear Science*, vol. 3, pp. 1–33, 1993.

[11] B. Owren and A. Marthinsen, "Runge-Kutta methods adapted to manifolds and based on rigid frames," *BIT Numerical Mathematics*, vol. 39, no. 1, pp. 116–142, 1999.

[12] H. Munthe-Kaas, "High order Runge-Kutta methods on manifolds," *Appl. Numer. Math.*, vol. 29, no. 1, pp. 115–127, 1999.

[13] E. Celledoni, A. Marthinsen, and B. Owren, "Commutator-free Lie group methods," *Future Generation Computer Systems*, vol. 19, no. 3, pp. 341–352, Abr. 2003.

[14] B. Owren, "Order conditions for commutator-free Lie group methods," *J. Phys. A: Math. Gen.*, vol. 39, pp. 5585–5599, 2006.

[15] J. Park and W.-K. Chung, "Geometric integration on Euclidean group with application to articulated multibody systems," *IEEE Transactions on Robotics*, vol. 21, no. 5, pp. 850–863, Oct. 2005.

[16] J. O. Smith and J. S. Abel, "The spherical interpolation method of source localization," *IEEE Journal of Oceanic Engineering*, vol. 12, no. 1, pp. 246–252, Jan. 1987.

[17] R. M. Murray, Z. Li, and S. S. Sastry, *A Mathematical Introduction to Robotic Manipulation*. CRC, 1994.

[18] S. P. Bhat and D. S. Bernstein, "A topological obstruction to continuous global stabilization of rotational motion and the unwinding phenomenon," *Systems and Control Letters*, vol. 39, no. 1, pp. 63–70, Jan. 2000.

[19] H. K. Khalil, *Nonlinear Systems*, 2nd ed. Prentice Hall, 1996.

[20] R. Burden and J. Faires, *Numerical Analysis*. Boston: PWS-KENT Publishing Company, 1993.